

# Experimental and Theoretical Approaches Toward Anion-Responsive Tripod–Lanthanide Complexes: Mixed-Donor Ligand Effects on Lanthanide Complexation and Luminescence Sensing Profiles

Yumiko Kataoka,<sup>[a]</sup> Dharam Paul,<sup>[a]</sup> Hiroyuki Miyake,<sup>[a]</sup> Tsuyoshi Yaita,<sup>[b]</sup> Eisaku Miyoshi,<sup>[c]</sup> Hirotoshi Mori,<sup>[c]</sup> Shinya Tsukamoto,<sup>[c]</sup> Hiroshi Tatewaki,<sup>[d]</sup> Satoshi Shinoda,<sup>[a]</sup> and Hiroshi Tsukube\*<sup>[a]</sup>

**Abstract:** A new series of tripods were designed to form anion-responsive, luminescent lanthanide complexes. These tripods contain pyridine, thiazole, pyrazine, or quinoline chromophores combined with amide carbonyl oxygen and tertiary nitrogen atoms. Crystallographic and EXAFS studies of the 10-coordinated tripod–La(NO<sub>3</sub>)<sub>3</sub> complexes revealed that each La<sup>3+</sup> cation was cooperatively coordinated by one tetradentate tripod and three bidentate NO<sub>3</sub><sup>−</sup> anions in the crystal and in CH<sub>3</sub>CN. Quantum chemical calculations indicat-

ed that the aromatic nitrogen plays a significant role in lanthanide complexation. The experimentally determined stability constants of complexes of the tripod with La(NO<sub>3</sub>)<sub>3</sub>, Eu(NO<sub>3</sub>)<sub>3</sub>, and Tb(NO<sub>3</sub>)<sub>3</sub> were in good agreement with the theoretically calculated interaction energies. Complexation of each tripod

with lanthanide triflate gave a mixture of several lanthanide complex species. Interestingly, the addition of a coordinative NO<sub>3</sub><sup>−</sup> or Cl<sup>−</sup> anion to the mixture significantly influenced the lanthanide complexation profiles. The particular combination of tripod and a luminescent Eu<sup>3+</sup> center gave anion-selective luminescence enhancements. Pyridine-containing tripods exhibited the highest NO<sub>3</sub><sup>−</sup> anion-selective luminescence and thus permit naked-eye detection of the NO<sub>3</sub><sup>−</sup> anion.

**Keywords:** anion sensing • density functional calculations • EXAFS spectroscopy • lanthanides • luminescence

## Introduction

On account of their intrinsic chemical, magnetic, and spectroscopic properties, specially designed lanthanide complexes are recognized as promising candidates for highly intelligent materials.<sup>[1]</sup> Some of these complexes function as asymmetric catalysts, biomedical probes, therapeutic medicines, and intense emitters. Because trivalent lanthanide cations have highly labile and versatile coordination features, functional sophistication of lanthanide complexes requires smart ligands to control their coordination structures.<sup>[2]</sup> Bünzli and co-workers developed triple-helicated heterobinuclear complexes, in which 3d metal and 4f lanthanide centers efficiently communicated with each other. Raymond et al. constructed three-dimensional cage-type lanthanide complexes as nanoscaled molecular vessels that effectively promoted bimolecular reactions. Shibasaki et al. characterized homopolymetallic lanthanide complexes supported by chiral tetradentate ligands for asymmetric catalysis. Luminescent lanthanide complexes have recently received attention.<sup>[3]</sup> Because of their long-lived, line-shaped, and posi-

[a] Dr. Y. Kataoka, Dr. D. Paul, Dr. H. Miyake, Dr. S. Shinoda, Prof. H. Tsukube  
Department of Chemistry, Graduate School of Science  
Osaka City University  
3-3-138 Sugimoto, Sumiyoshi-ku, Osaka 558-8585 (Japan)  
Fax: (+81) 6-6605-2560  
E-mail: tsukube@sci.osaka-cu.ac.jp

[b] Dr. T. Yaita  
Actinide Coordination Chemistry Group  
Synchrotron Radiation Research Center  
Quantum Beam Science Directorate, Japan Atomic Energy Agency  
1-1-1 Koto, Sayo-cho, Sayo-gun, Hyogo 679-5148 (Japan)

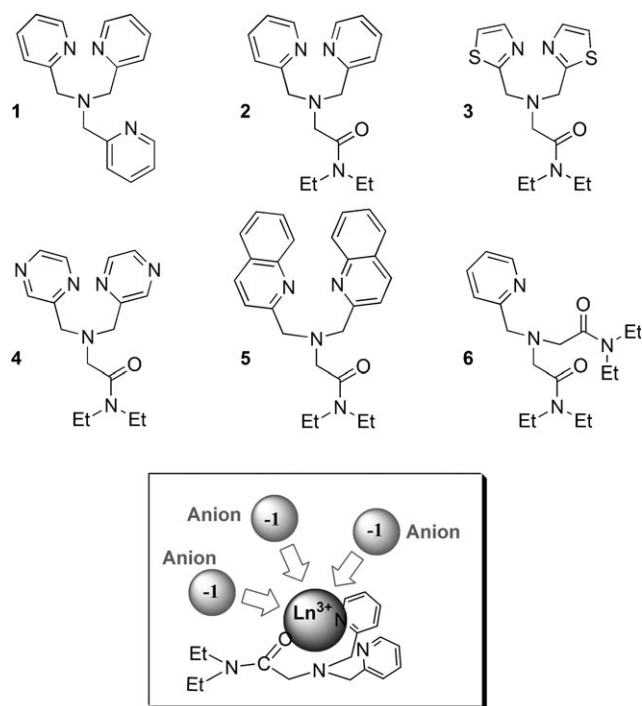
[c] Prof. E. Miyoshi, Dr. H. Mori, S. Tsukamoto  
Graduate School of Engineering Science, Kyushu University  
6-1 Kasuga-Park, Fukuoka 816-8580 (Japan)

[d] Prof. H. Tatewaki  
Department of Information and Biological Sciences  
Graduate School of Natural Sciences, Nagoya City University  
1 Yamanohata, Mizuho-cho, Mizuho-ku, Nagoya  
Aichi 467-8501 (Japan)

Supporting information for this article is available on the WWW under <http://www.chemeurj.org/> or from the author.

tion-defined luminescence, they have been successfully applied to nonradioactive labeling of biomolecules, naked-eye detection of inorganic anions, and biotargeted imaging processes. Parker et al. combined heptadentate 1,4,7,10-tetra-cyclododecane (cyclen) ligands with a  $\text{Eu}^{3+}$  center to form effective lanthanide complexes for in vivo and in vitro anion detection. Ziessel et al. employed luminescent lanthanide complexes with bis-bipyridine phosphine oxide ligands for biopolymer tagging. Vögtle et al. and Petoud et al. further developed dendrimer–lanthanide complexes as intense near-infrared emitters.<sup>[4]</sup> These sophisticated ligands elegantly generated outstanding lanthanide complex functions, but their structures were too complicated to be modified. Although there have been many experimental approaches to control the coordination numbers, versatile stoichiometry, and rapid dynamics of lanthanide complexes, most of the reported complexes were coordinatively unsaturated and often present as mixtures of polynuclear, highly ordered, hydrated, and oxo-bridged complexes in solution.<sup>[5]</sup>

We have previously demonstrated that tris(2-pyridylmethyl)amine (**1**) and its chiral derivatives formed luminescent  $\text{Eu}^{3+}$  and  $\text{Tb}^{3+}$  complexes.<sup>[5b,c]</sup> Based on the dynamic and unsaturated coordination features, the tripod–lanthanide complexes had several coordination sites available for external coordinative anions and exhibited anion-responsive luminescence profiles. We present below a new series of mixed-donor tripods **2–6** for lanthanide complexation (Scheme 1). The donor effects of the tripods on lanthanide complexation and the luminescence profile were characterized by crystal structure determinations, UV/Vis and NMR spectroscopy titrations, and luminescence experiments. The



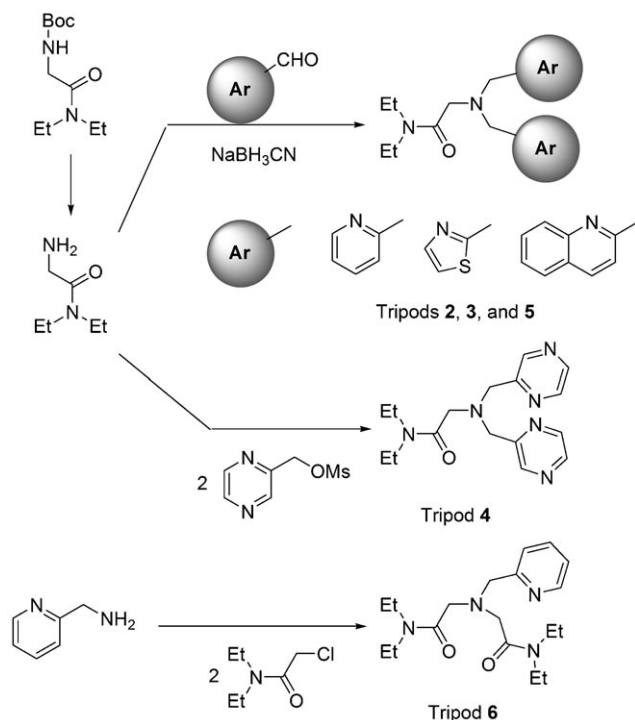
Scheme 1. Structures of tripods and lanthanide complexation.

mixed-donor tripods predominantly formed 10-coordinated complexes with lanthanide nitrates in a 1:1:3 (tripod/lanthanide cation/anion) stoichiometry. Furthermore, they were characterized by EXAFS structural analysis and quantum chemical calculations. Although such EXAFS analysis and quantum chemical calculations have been examined in a limited number of lanthanide complex systems,<sup>[6]</sup> our combined studies of experimental and theoretical approaches demonstrate that tripods can be structurally optimized to form anion-responsive, luminescent lanthanide complexes.

## Results and Discussion

**Synthesis of the tripods:** Various tripods incorporating phosphorus donors, pyrazoyl groups, alkoxides, triamines, triamides, tripyridines, and other coordinating groups have already been prepared for lanthanide complexation.<sup>[7]</sup> Among them, several tripods with aromatic nitrogen atoms have been reported to form 10-coordinated complexes with lanthanide chlorides and nitrates. Crystallographic studies of these complexes revealed that the lanthanide centers were three-dimensionally shielded from solvents and exhibited intense lanthanide luminescence.<sup>[7,8]</sup> In addition to 1:1:3 complexes, these tripods often gave mixtures containing 2:1 and 3:1 (tripod/lanthanide cation) complexes as well as hydrated mononuclear and oxo-bridged binuclear species.<sup>[5,9,10]</sup> For this reason, an effective approach is required to control the versatile coordination structure of the tripods for efficient development of luminescent lanthanide complexes.

We combined one or two aromatic nitrogen moieties, such as pyridine, thiazole, pyrazine, or quinoline, with glycine amide in a tripod skeleton (**2–6** in Scheme 1).<sup>[10]</sup> The aromatic nitrogen moieties can provide “soft” coordination with the lanthanide centers and also act as effective photo-antennae for excitation of the lanthanide cations.<sup>[11]</sup> Karmazin et al. compared 4f/5f metal complexation properties of **1** and its derivatives with three aromatic nitrogen moieties,<sup>[12]</sup> and observed significant donor effects of the aromatic nitrogen atoms. The introduced amide group is expected to function as a “hard” donor for lanthanide cations and provide comparable stability constants of lanthanide complexes to those with aromatic nitrogen atoms.<sup>[10b,13]</sup> These mixed-donor tripods further form dissymmetric lanthanide complexes. As indicated by Nakamura et al., such dissymmetric complexes can exhibit more intense lanthanide luminescence than the corresponding symmetric tripod complexes.<sup>[14]</sup> Because sufficient space is available around the coordinating amide group for incoming guest species, the mixed-donor tripods are expected to form highly coordinated, structurally defined complexes that exhibit anion-responsive luminescence functions. The synthetic routes of the tripods were simple and straightforward as illustrated in Scheme 2. Tripods **2**, **3**, and **5** were derived from glycine amide and the corresponding formyl-substituted aromatic nitrogen compound. Tripod **2**, which contains two pyridine rings, was typically prepared by repeated Schiff base forma-



Scheme 2. Synthetic routes to tripods 2–6.

tion of diethyl glycine amide with formylpyridine and hydrogenation with  $\text{NaBH}_3\text{CN}$ . Tripod **4** was obtained by treating pyrazine-ethanol mesylate with glycine amide, whereas tripod **6** was synthesized by treating 2-aminomethylpyridine with excess diethyl chloroacetamide. The new ligands were fully characterized by  $^1\text{H}$  and  $^{13}\text{C}$  NMR, and IR spectroscopies; HRMS; and elemental analysis.

**Crystal and optimized structures of tripod–lanthanide complexes:** Mazzanti et al. determined the crystal structure of the  $[\text{Eu}(\mathbf{1})\text{Cl}_3]$  (1:1:3) complex, in which four nitrogen atoms from the tripod and three  $\text{Cl}^-$  anions cooperatively coordinate to the  $\text{Eu}^{3+}$  center.<sup>[7b]</sup> Wong et al. isolated similar 1:1 lanthanide complexes with related tripods.<sup>[8]</sup> We determined the crystal structure of the  $[\text{La}(\mathbf{2})(\text{NO}_3)_3]$  (1:1:3) complex in which no water or solvent molecule was included in the coordination sphere. As illustrated in Figure 1a, three nitrogen

atoms and one carbonyl oxygen atom in the tripod cooperatively coordinate to the  $\text{La}^{3+}$  center along with three bidentate  $\text{NO}_3^-$  anions to form a complex with a total coordination number of 10. Tripod **5** has been demonstrated to form a similar 10-coordinated complex with  $\text{La}(\text{NO}_3)_3$ .<sup>[10b]</sup> Table 1 compares the  $\text{La}-\text{N}_{\text{arom}}$  bond lengths in a crystal of the  $[\text{La}(\mathbf{2})(\text{NO}_3)_3]$  complex (2.680(4) and 2.739(4) Å) with those of a crystal of  $[\text{La}(\mathbf{5})(\text{NO}_3)_3]$  (2.772(2) and 2.825(2) Å). Because the former bond lengths are significantly shorter than the latter, we conclude that the pyridine nitrogen atom coordinates more strongly than that of quinoline in our tripod framework. The  $\text{La}-\text{N}_{\text{amine}}$  and  $\text{La}-\text{O}_{\text{amide}}$  bond lengths of these two isolated complexes exhibited slight differences. As described below, the amide oxygen atom was found to have a higher charge distribution than either of the two types of nitrogen atoms, and the  $\text{La}-\text{O}_{\text{amide}}$  bond lengths determined in the two tripod complexes are short. These two complexes included three bidentate  $\text{NO}_3^-$  anions in somewhat different fashions. Because tripod **5** led to a less symmetric arrangement of the three  $\text{NO}_3^-$  anions compared with tripod **2**, the quinoline moieties may cause more severe steric hindrance in the anion coordination process than the pyridine moieties. Thus, these mixed-donor tripods offered characteristic tetradentate coordination for lanthanide cations.

Because the tripods have flexible and dynamic coordination modes, lanthanide tripod complexes often have different coordination structures in solutions and in the crystal. Figure 2a and b compare the radial structural functions

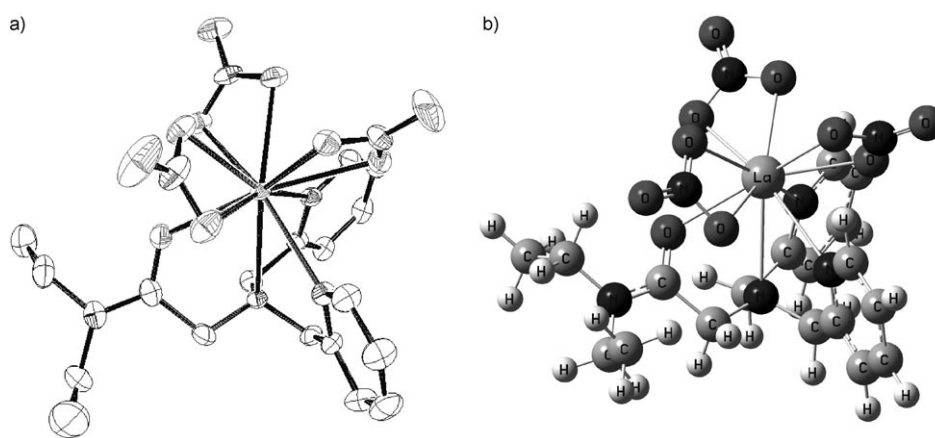


Figure 1. Crystal (a) and optimized (b) structures of the  $[\text{La}(\mathbf{2})(\text{NO}_3)_3]$  complex. Thermal ellipsoids in the crystal structure are drawn at the 50% probability level, and all hydrogen atoms and solvent acetonitrile molecules are omitted for clarity.

Table 1. Bond lengths and charge distributions of tripod– $\text{La}(\text{NO}_3)_3$  (1:1:3) complexes.

	Bond length [Å] <sup>[a]</sup>			Charge distribution <sup>[b]</sup>		
	$\text{La}-\text{N}_{\text{arom}}$	$\text{La}-\text{N}_{\text{amine}}$	$\text{La}-\text{O}_{\text{amide}}$	$\text{N}_{\text{arom}}$	$\text{N}_{\text{amine}}$	$\text{O}_{\text{amide}}$
<b>2</b>	2.782, 2.929 (2.680, 2.739)	2.955 (2.738)	2.652 (2.465)	−0.509, −0.511	−0.522	−0.697
<b>3</b>	2.753, 2.887	3.117	2.624	−0.516, −0.520	−0.526	−0.696
<b>4</b>	2.743, 2.852	2.909	2.557	−0.468, −0.471	−0.525	−0.697
<b>5</b>	2.784, 2.891 (2.772, 2.825)	2.906 (2.714)	2.645 (2.426)	−0.510, −0.516	−0.516	−0.699

[a] B3LYP (Stuttgart-RSC-ECP;  $\text{La} + \text{cc-pVDZ}$ ; C, N, O, and H) results. The values in parentheses are experimental results from the isolated crystals. [b] IEFPCM/B3LYP (Stuttgart-RSC-ECP;  $\text{La} + \text{cc-pVDZ}$ ; C, N, O, and H) results. Calculated as the free ligands in  $\text{CH}_3\text{CN}$ .

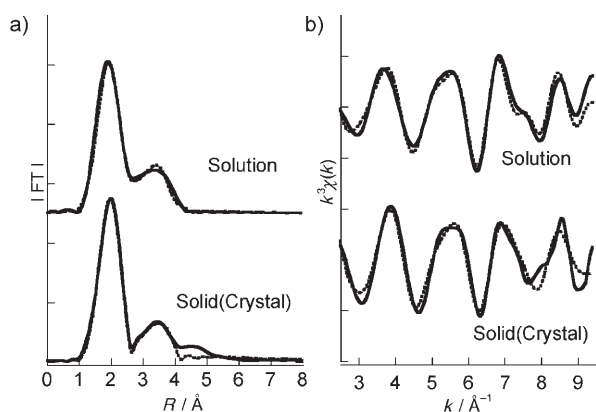


Figure 2. a) Radial structural functions of the  $[\text{La}(\mathbf{2})(\text{NO}_3)_3]$  complex in a  $\text{CH}_3\text{CN}$  solution and in the crystal. Phase shifts were not corrected. FT ranges:  $3.5\text{--}9.5 \text{ \AA}^{-1}$ . b) EXAFS oscillations. Solid and dashed lines denote experimental and calculated data, respectively.

(RSF) and the  $k^3$ -weight EXAFS oscillations of the  $[\text{La}(\mathbf{2})(\text{NO}_3)_3]$  (1:1:3) complex in  $\text{CH}_3\text{CN}$  and in the crystal. Two significant peaks were observed in the RSF curves. The crystal structure included disorder in the bond length in the primary coordination sphere, and the number of backscattering interactions was considered to be two or three for the first peaks and two for the second peaks during the fitting process. The curve-fitting results (dashed lines) agreed well with the raw data for the RSF and the EXAFS oscillations. The data for the estimated coordination number ( $N$ ), bond length ( $R$ ), and squared Debye–Waller factor ( $\sigma^2$ ) are listed in Table 2. The shortest interaction found in the crystal data

Table 2. EXAFS fitting results of the  $[\text{La}(\mathbf{2})(\text{NO}_3)_3]$  complex in the crystal and in a  $\text{CH}_3\text{CN}$  solution.<sup>[a]</sup>

	$N$	Crystal		in $\text{CH}_3\text{CN}$		
		$R[\text{\AA}]$	$\sigma^2[\text{\AA}^2]$	$N$	$R[\text{\AA}]$	$\sigma^2[\text{\AA}^2]$
La–O <sub>amide</sub>	1	2.47	0.01			
La–O <sub>nitrate</sub> , La–O <sub>amide</sub> <sup>[b]</sup>	7	2.59	0.02	8	2.56	0.02
La–N <sub>arom</sub>	2	2.74	0.01	2	2.71	0.02
La–C <sub>arom</sub>	8	3.52	0.03	8	3.61	0.03
La–N–O	6	4.26	0.02	6	4.22	0.02

[a]  $N$ : coordination number (first decimal place rounded off);  $R$ : bond distance;  $\sigma^2$ : Debye–Waller factor. The fitting qualities for all the data were less than  $r=25\%$ ;  $r$ : residual =  $|\sum |y_{\text{exp}(i)} - y_{\text{theo}(i)}| / \sum |y_{\text{exp}(i)}| \times 100 [\%]$ . [b] This bond length was estimated in solution.

arising from La–O<sub>amide</sub> scattering was not taken into account in fitting the solution data. The La–O<sub>nitrate</sub> bond length of the sample in solution was slightly shorter than that of the crystal, which suggests that dynamic averaging and rearrangement of the ligands in the primary coordination sphere occurred in the solution state. Because the RSF and EXAFS oscillation curves obtained in the solution state had almost the same shapes and peak positions as those obtained in the solid state, it was confirmed that the  $[\text{La}(\mathbf{2})(\text{NO}_3)_3]$  complex maintained its 10-coordinated structure in  $\text{CH}_3\text{CN}$ . Interestingly, all of the  $\text{NO}_3^-$  anions were nicely accommodated, as

observed in the crystal state, and were rarely displaced by solvent and water molecules.

Quantum chemical calculations were performed to characterize the tripod– $\text{La}(\text{NO}_3)_3$  (1:1:3) complexes from a theoretical point of view. We optimized the geometry of each complex using density functional B3LYP, in which the initial geometries were generated from the experimentally determined crystal structures of the  $[\text{La}(\mathbf{2})(\text{NO}_3)_3]$  and  $[\text{La}(\mathbf{5})(\text{NO}_3)_3]$  complexes. The integral equation formalism polarized continuum model (IEFPCM)<sup>[15]</sup> was used to consider the  $\text{CH}_3\text{CN}$  solvent effect. Figure 1 compares the optimized and crystal structures of the  $[\text{La}(\mathbf{2})(\text{NO}_3)_3]$  complex: both have very similar 10-coordinated modes. Table 1 lists the bond lengths of the optimized  $\text{La}(\text{NO}_3)_3$  complexes with tripods  $\mathbf{2}\text{--}\mathbf{5}$ , and Figure S1 in the Supporting Information illustrates their optimized structures. Natural charge distributions were calculated from an NBO analysis<sup>[16]</sup> of tripod fragments for the optimized geometries of the tripod– $\text{La}(\text{NO}_3)_3$  complexes (Table 1). The amide oxygen atom of each tripod was found to be a more effective binding site than either type of nitrogen atom.<sup>[10b,13]</sup> In the structurally optimized complexes, La–N<sub>amine</sub> bonds were longer than La–N<sub>arom</sub> bonds, and tripod  $\mathbf{3}$  had the longest La–N<sub>amine</sub> bond. A comparison of the charge distributions in the aromatic nitrogen moieties showed that the nitrogen atom of thiazole was the most electron-rich and the pyrazine nitrogen atom coordinated most weakly with the  $\text{La}^{3+}$  cation. These quantum calculation results did not directly relate to the experimentally determined stability constants, as described below. This suggests that a suitable arrangement of the tetradentate donors can stabilize the tripod–lanthanide complex.

**Lanthanide complexation in  $\text{CH}_3\text{CN}$  solutions:** Figure 3 shows the  $^1\text{H}$  NMR spectra of tripod  $\mathbf{2}$  upon complexation with  $\text{La}(\text{NO}_3)_3$  and  $\text{La}(\text{CF}_3\text{SO}_3)_3$  in  $\text{CD}_3\text{CN}$ . These spectra indicate that the two  $\text{La}^{3+}$  salts exhibit somewhat different complexation behavior. When tripod  $\mathbf{2}$  formed complexes with  $\text{La}(\text{NO}_3)_3$ , several broad signals appeared at a molar ratio of  $[\text{La}^{3+}]/[\mathbf{2}] = 0.33$  and  $0.50$ , in addition to the signals assigned to the free and 1:1 complex species (Figure 3b and c). Although the employed  $\text{CD}_3\text{CN}$  solutions contained  $6.0 \times 10^{-3}$  or  $1.0 \times 10^{-2} \text{ mol L}^{-1}$  of  $\text{H}_2\text{O}$ , an equimolar mixture of  $\text{La}(\text{NO}_3)_3$  and tripod  $\mathbf{2}$  gave a crystal of the non-hydrated 10-coordinated complex illustrated in Figure 1a. The unassigned signals completely disappeared at  $[\text{La}^{3+}]/[\mathbf{2}] = 1.0$ , and only the peaks for the 1:1 complex remained at  $[\text{La}^{3+}]/[\mathbf{2}] \geq 1.0$  (Figure 3d and e). Mazzanti et al. determined the crystal structures of 1:1 and 2:1 complexes of ligand  $\mathbf{1}$  and its derivatives with lanthanide chlorides and nitrates; hydroxo complexes were also isolated.<sup>[5a,7b]</sup> Thus, tripod  $\mathbf{2}$  forms an equilibrium mixture of  $\text{La}^{3+}$  complexes that had slightly slower kinetics than the NMR spectroscopy time-scale. ESI-MS measurements supported the formation of 2:1 and 1:1 complexes with lanthanide nitrates. When  $\text{Tb}(\text{NO}_3)_3$  was mixed with an equimolar quantity of tripod  $\mathbf{2}$  in  $\text{CH}_3\text{CN}$ , peaks assigned to  $[\text{Tb}^{3+} + 2\mathbf{2} + 2\text{OH}^- + \text{CH}_3\text{CN} + 3\text{H}_2\text{O}]^{2+}$  and  $[\text{Tb}^{3+} + 2\mathbf{2} + 2\text{NO}_3^-]^+$  were detected at  $m/z$  912

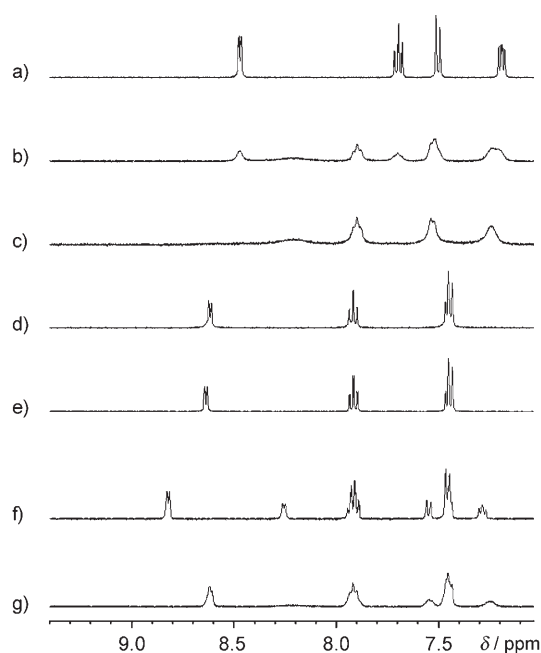


Figure 3.  $^1\text{H}$  NMR titrations of  $\text{La}^{3+}$  complexation of tripod **2**. [Tripod **2**] =  $4.0 \times 10^{-4}$  mol L $^{-1}$ ; a) no  $\text{La}^{3+}$  salt, b) 0.33 equiv [ $\text{La}(\text{NO}_3)_3$ ], c) 0.50 equiv [ $\text{La}(\text{NO}_3)_3$ ], d) 1.0 equiv [ $\text{La}(\text{NO}_3)_3$ ], e) 2.0 equiv [ $\text{La}(\text{NO}_3)_3$ ], f) 1.0 equiv [ $\text{La}(\text{OTf})_3$ ], g) 1.0 equiv [ $\text{La}(\text{OTf})_3$ ], 3.0 equiv [ $n\text{Bu}_4\text{N}(\text{NO}_3)$ ].

and 595 (Figure S2 in the Supporting Information). In contrast, an equimolar mixture of tripod **2** and  $\text{La}(\text{CF}_3\text{SO}_3)_3$  gave a somewhat complicated  $^1\text{H}$  NMR spectrum, which indicated that other complex species were formed in addition to the 1:1 complex that had a more static nature (Figure 3f). Addition of further tetrabutylammonium nitrate to this mixture gave more broad signals in the  $^1\text{H}$  NMR spectrum (Figure 3g). Because the added  $\text{NO}_3^-$  anion accelerated interconversion between the resulting complex species, tripod **2** exhibited anion-dependent lanthanide complexation behavior in solutions.

The complexation behavior of tripods **2–5** with lanthanide nitrates were quantitatively characterized by monitoring UV/Vis absorption changes of the aromatic nitrogen moiety. When these changes were plotted against the added amount of  $\text{La}(\text{NO}_3)_3$ ,  $\text{Eu}(\text{NO}_3)_3$ , or  $\text{Tb}(\text{NO}_3)_3$ , each titration curve gave a good fit for a mixture of 1:1 and 2:1 complexes (Figure S3 in the Supporting Information). However, the spectral changes observed with tripod **6** were too small to use in the determination of the complex stability constant. Table 3 lists the estimated  $\log K_1$  and  $\log K_2$  values for  $\text{La}(\text{NO}_3)_3$ ,  $\text{Eu}(\text{NO}_3)_3$ , and  $\text{Tb}(\text{NO}_3)_3$  in  $\text{CH}_3\text{CN}$ . Tripods **2** and **4** had similar  $\log K_1$  values for the three lanthanide nitrates, but tripods **3** and **5** formed more stable complexes with  $\text{La}(\text{NO}_3)_3$  than with  $\text{Eu}(\text{NO}_3)_3$  and  $\text{Tb}(\text{NO}_3)_3$ . Although the observed  $\log K_1$  and  $\log K_2$  values were lower than the values for caged cryptand[2.2.2] ( $\log K = 10.8$  for  $\text{La}^{3+}$  complex in  $\text{CH}_3\text{CN}$ ),<sup>[17]</sup> the tripods formed lanthanide complexes that were sufficiently stable to be used at luminescence concentrations.

Table 3. Stability and luminescence profiles of lanthanide nitrate complexes with tripods **2–5**.

	Stability constants <sup>[a]</sup>			I.E. <sup>[b]</sup> $\text{La}^{3+}$	Luminescence <sup>[c]</sup>		
	$\text{La}^{3+}$	$\text{Eu}^{3+}$	$\text{Tb}^{3+}$		$\text{Eu}^{3+}$	$\alpha$ <sup>[d]</sup>	$\text{Tb}^{3+}$
					lifetime [ms]	lifetime [ms]	
<b>2</b>	$5.7 \pm 0.1$ <i><math>4.7 \pm 0.1</math></i>	$5.5 \pm 0.1$ <i><math>3.9 \pm 0.1</math></i>	$5.5 \pm 0.1$ <i><math>3.9 \pm 0.1</math></i>	-89.1	1.5	5.5	1.9
<b>3</b>	$6.9 \pm 0.1$ <i><math>4.9 \pm 0.1</math></i>	$5.9 \pm 0.3$ <i><math>4.3 \pm 0.2</math></i>	$6.2 \pm 0.4$ <i><math>4.5 \pm 0.4</math></i>	-99.9	1.5	6.7	1.9
<b>4</b>	$6.5 \pm 0.3$ <i><math>4.8 \pm 0.1</math></i>	$6.7 \pm 0.3$ <i><math>4.8 \pm 0.1</math></i>	$6.7 \pm 0.2$ <i><math>4.8 \pm 0.1</math></i>	-92.8	1.4	5.7	1.9
<b>5</b>	$6.4 \pm 0.1$ <i><math>3.1 \pm 0.1</math></i>	$5.5 \pm 0.2$ <i><math>4.2 \pm 0.1</math></i>	$5.5 \pm 0.1$ <i><math>4.3 \pm 0.1</math></i>	-93.6	1.1	10	– <sup>[e]</sup>

[a]  $\log K_1$  values are shown in normal text and  $\log K_2$  values are shown in italic text. [b] I.E.: interaction energy. The level of density functional theory used in the calculations was B3LYP (Stuttgart-RSC-ECP;  $\text{La} + \text{cc-pVDZ}$ ; C,N,O, and H). [c] Measured with tripod– $\text{Ln}(\text{NO}_3)_3$  (1:1) complexes (25 °C,  $\text{CH}_3\text{CN}$ ). [d]  $\alpha = [\text{Eu}^{3+}$  emission intensity at 616 nm]/[ $\text{Eu}^{3+}$  emission intensity at 592 nm]. [e] Too weak to be determined.

The processes involved in tripod–lanthanide complexation were further characterized from a theoretical point of view, even though a limited number of quantum chemical calculations have been attempted in previous lanthanide complex characterization.<sup>[6c–f]</sup> The interaction energy (I.E.), as defined in Equation (1), was theoretically calculated for a series of tripod– $\text{La}(\text{NO}_3)_3$  complexes as a measure of the complex stability.

$$\text{I.E.} = E[\text{tripod} - \text{La}^{3+} - (\text{NO}_3)_3] - (E[\text{La}(\text{NO}_3)_3 \text{ fragment}] + E[\text{tripod fragment}]) \quad (1)$$

In this equation,  $E[\text{tripod} - \text{La}^{3+} - (\text{NO}_3)_3]$ ,  $E[\text{La}(\text{NO}_3)_3 \text{ fragment}]$ , and  $E[\text{tripod fragment}]$  represent the density functional B3LYP total energy of the optimized tripod– $\text{La}^{3+} - (\text{NO}_3)_3$  complexes and their components, the  $\text{La}(\text{NO}_3)_3$  and the tripod fragments at the tripod– $\text{La}^{3+} - (\text{NO}_3)_3$  optimized point, respectively. The calculated I.E. values for the four tripod– $\text{La}(\text{NO}_3)_3$  complexes are compared with the experimentally determined stability constants in Table 3. Although tripod **3** exhibited a larger  $\log K_1$  value with  $\text{La}(\text{NO}_3)_3$  than tripod **2**, **4**, or **5** in the titration experiments, the calculation of I.E. values revealed a comparable trend: tripod **2** < tripod **5**  $\approx$  tripod **4** < tripod **3**. Because the calculation results suggest that tripod **3** has the most negative charge distribution for the  $\text{N}_{\text{arom}}$  atoms, but the longest  $\text{La} - \text{N}_{\text{amine}}$  bond length, the three-dimensional arrangement of the four donor atoms essentially determined the stability of the tripod–lanthanide complex.

**Luminescence profiles of tripod–lanthanide complexes:** Lanthanide luminescence is a phenomenon that is very sensitive to the coordination environment around the lanthanide center.<sup>[3,11]</sup> The present type of mixed-donor tripods operated as coordinatively unsaturated ligands to form anion-responsive, luminescent lanthanide complexes with particular anions.<sup>[5]</sup> Since additional coordination from the external anion often alters the stoichiometry, geometry, and structure

of the ternary “tripod-lanthanide-anion” complex,<sup>[10b]</sup> a new luminescence-based anion-sensing process can be constructed.

$\text{Eu}^{3+}$  and  $\text{Tb}^{3+}$  complexes with tripods **2–6** showed characteristic lanthanide emissions through ligand excitation and subsequent ligand-to-metal energy-transfer processes. Figure 4 illustrates the typical luminescence spectra of equi-

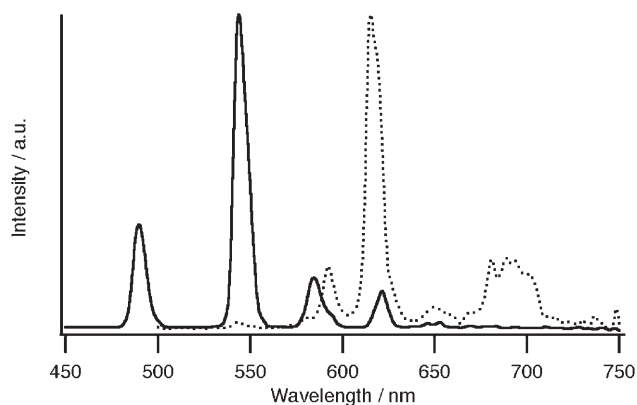


Figure 4. Corrected luminescence spectra of tripod  $[\text{Tb}(\mathbf{2})(\text{NO}_3)_3]$  (—) and  $[\text{Eu}(\mathbf{2})(\text{NO}_3)_3]$  (----) complexes in  $\text{CH}_3\text{CN}$ . Conditions: [tripod **2**] =  $[\text{Ln}(\text{NO}_3)_3] = 5.0 \times 10^{-6} \text{ mol L}^{-1}$ ; RT;  $\lambda_{\text{ex}} = 261 \text{ nm}$ ; emission slit, 2.5 nm.

molar mixtures of  $\text{Eu}(\text{NO}_3)_3$  and  $\text{Tb}(\text{NO}_3)_3$  with tripod **2** in  $\text{CH}_3\text{CN}$ , in which 1:1:3 complexes predominantly formed. As summarized in Table 3, the series of tripod- $\text{Eu}^{3+}$  complexes showed shorter lifetimes than the corresponding  $\text{Tb}^{3+}$  complexes. The relative intensities ( $\alpha$  values) of the  $\text{Eu}^{3+}$  emission bands at 616 nm and 592 nm are compared as indications of the complex symmetries.<sup>[18]</sup> Tripods **2–4** exhibited similar luminescence lifetimes and  $\alpha$  values of lanthanide nitrate complexes; however, tripod **5**, which has 2-quinoline groups, gave a larger  $\alpha$  value and shorter lifetime than the others. Thus, the nature of the introduced aromatic nitrogen moieties influenced not only complex stability but also the  $\text{Eu}^{3+}$  complex symmetry.

**Anion-sensing application of luminescent lanthanide complexes:** We previously reported that tripod **1** and the  $\text{Eu}(\text{CF}_3\text{SO}_3)_3$  system was effective as a luminescent sensory device specific for  $\text{NO}_3^-$  anion detection, whereas the corresponding  $\text{Tb}^{3+}$  complex system exhibited modest  $\text{Cl}^-$  anion-responsive luminescence.<sup>[5b]</sup> The fact that coordination from additional anions significantly influenced the structures of the present tripod-lanthanide complexes provided a promising possibility for the development of new luminescence-based anion-sensing processes. When tripod **2, 3, 4, 5, or 6** was mixed with an equimolar quantity of  $\text{Eu}(\text{CF}_3\text{SO}_3)_3$  in  $\text{CH}_3\text{CN}$  ( $5 \times 10^{-6} \text{ mol L}^{-1}$ ), excitation of the ligand chromophore resulted in a characteristic  $\text{Eu}^{3+}$  luminescence spectrum. Addition of further tetrabutylammonium salt containing the  $\text{I}^-$ ,  $\text{Br}^-$ ,  $\text{Cl}^-$ ,  $\text{F}^-$ ,  $\text{ClO}_4^-$ ,  $\text{NO}_3^-$ ,  $\text{CH}_3\text{CO}_2^-$ ,  $\text{SCN}^-$ ,  $\text{HSO}_4^-$ , or  $\text{H}_2\text{PO}_4^-$  anion induced anion-dependent changes in the luminescence spectra (Figure 5).

When the  $2\text{-Eu}^{3+}$  complex system was typically employed, the observed luminescence intensity at 616 nm increased four-fold on addition of three equivalents of  $\text{NO}_3^-$ , whereas the addition of other anions gave slight enhance-

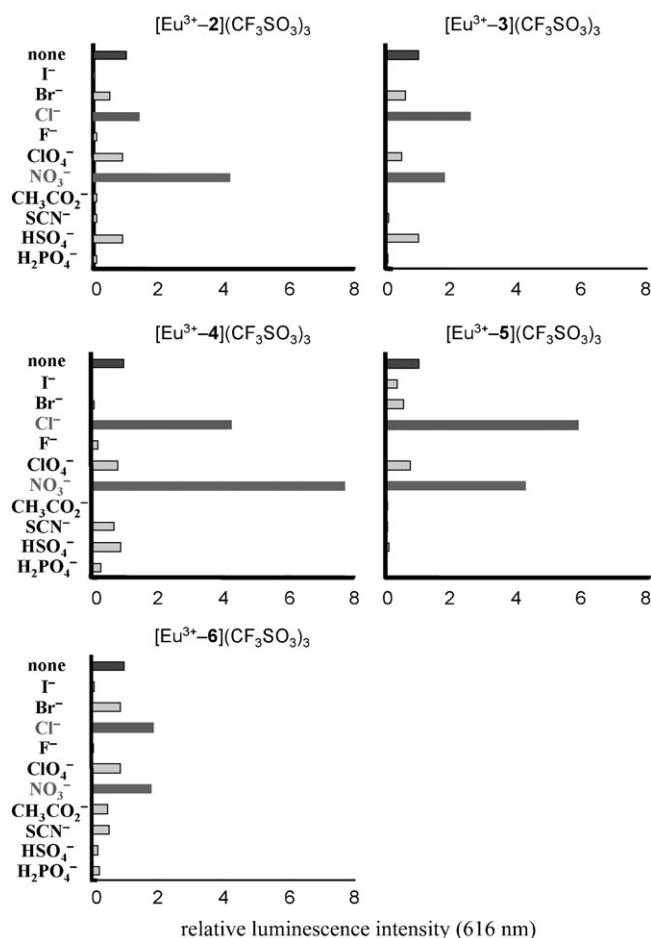


Figure 5. Anion-sensing profiles of luminescent tripod- $\text{Eu}^{3+}$  complexes.  $[\text{Eu}(\text{CF}_3\text{SO}_3)_3] = 5.0 \times 10^{-6} \text{ mol L}^{-1}$ ; [tripod] =  $5.0 \times 10^{-6} \text{ mol L}^{-1}$ ; **2**: excitation at 261 nm, slit widths 10/5 nm; **3**: excitation at 246 nm, slit widths 10/5 nm; **4**: excitation at 270 nm, slit widths 10/3 nm; **5**: excitation at 305 nm, slit widths 10/7 nm; **6**: excitation at 264 nm, slit widths 10/5 nm;  $[\text{nBu}_4\text{NX}] = 1.5 \times 10^{-5} \text{ mol L}^{-1}$ .

ments ( $< 1.5$ -fold). As the  $\text{NO}_3^-$  anion concentration increased, the intensity of the observed luminescence was proportionally enhanced and was saturated at  $[\text{NO}_3^-]/[\text{Eu}^{3+}] = 3$ . As described above, the equimolar mixture of tripod **2** and  $\text{Eu}(\text{CF}_3\text{SO}_3)_3$  gave a mixture of several complex species, but the added  $\text{NO}_3^-$  anion was supported to promote the formation of the highly luminescent 1:1:3 complex, in which the  $\text{NO}_3^-$  anions occupied the three exchangeable coordination sites of the  $\text{Eu}^{3+}$  center and prevented quenching by means of solvation. In contrast, the addition of the non-coordinative  $\text{ClO}_4^-$  anion to the  $2\text{-Eu}(\text{CF}_3\text{SO}_3)_3$  complex system induced no significant change in the UV/Vis and luminescence spectra, whereas the addition of  $\text{F}^-$  and  $\text{CH}_3\text{CO}_2^-$  anions decomposed the tripod-lanthanide com-

plexes themselves. Thus, the  $2\text{-Eu}^{3+}$  complex showed the largest  $\text{NO}_3^-$  anion-responsive luminescence enhancement, which was applicable to naked eye detection at  $10^{-5} \text{ mol L}^{-1}$  level (Figure 6).

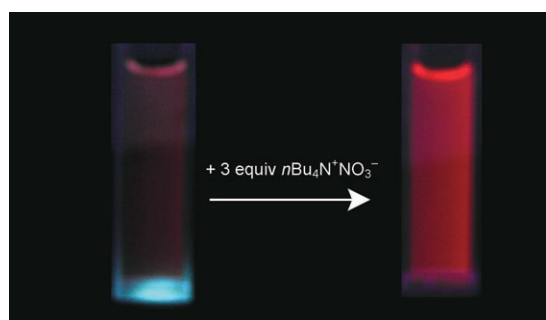


Figure 6. Naked-eye detection of the  $\text{NO}_3^-$  anion with the  $2\text{-Eu}^{3+}$  complex. The pictures were taken under the following conditions:  $[2] = 5.0 \times 10^{-6} \text{ mol L}^{-1}$ ;  $[\text{Eu}(\text{CF}_3\text{SO}_3)_3] = 5.0 \times 10^{-6} \text{ mol L}^{-1}$ ;  $[\text{nBu}_4\text{N}(\text{NO}_3)] = 1.5 \times 10^{-5} \text{ mol L}^{-1}$ ; in  $\text{CH}_3\text{CN}$ . A UV TLC detection lamp (4 W) was used for the excitation.

Tripods **3–6** exhibited different anion-response luminescence-sensing profiles. An equimolar mixture of  $\text{Eu}(\text{CF}_3\text{SO}_3)_3$  and tripod **4** or **5** exhibited enhanced luminescence upon addition of both  $\text{Cl}^-$  and  $\text{NO}_3^-$  anions. Because these two anions gave similar luminescence enhancements, the anion selectivity of these tripod complexes was modest. The luminescence of the  $\text{Eu}^{3+}$  complexes with tripods **3** and **6** was slightly enhanced on addition of a series of anions, which indicated that the nature of the tripod used has a significant influence on the anion-sensing profile of the resulting  $\text{Eu}^{3+}$  complex. The luminescence lifetimes of  $\text{Eu}^{3+}$  complexes with tripods **2** and **4** were significantly enhanced by the addition of  $\text{NO}_3^-$  and moderately by the addition of  $\text{Cl}^-$ :  $2\text{-Eu}^{3+}$ , 1.5 ms for  $\text{NO}_3^-$  and 1.2 ms for  $\text{Cl}^-$ ; and  $4\text{-Eu}^{3+}$ , 1.5 ms for  $\text{NO}_3^-$  and 1.1 ms for  $\text{Cl}^-$ .<sup>[19]</sup> When  $\text{Tb}(\text{CF}_3\text{SO}_3)_3$  was combined with these tripods, the observed  $\text{Tb}^{3+}$  luminescence signals were changed slightly by addition of external guest anions, and the largest observed enhancement in the intensity was only 1.5-fold for a combination of tripod **4**,  $\text{Tb}^{3+}$  cation, and  $\text{NO}_3^-$  anion. Thus, the  $2\text{-Eu}^{3+}$  complex offered the most effective and selective luminescence-based anion-sensing.

## Conclusion

A new series of tripod–lanthanide complexes were fully characterized by crystallographic and EXAFS examinations, UV/Vis and NMR spectroscopy titration experiments, stability constant estimations, quantum chemical calculations, and anion-responsive luminescence measurements. The combined studies of experimental and theoretical characterizations demonstrated that the present type of mixed-donor tripods possess both effective chromophores for intense lanthanide luminescence and potential coordination sites for

external anions. Although their lanthanide complexes can have versatile coordination structures in  $\text{CH}_3\text{CN}$ , the tripod  $2\text{-La}(\text{NO}_3)_3$  complex maintained a 10-coordinated structure both in the crystal and in  $\text{CH}_3\text{CN}$ . The addition of coordinative anions specifically promoted the formation of luminescent  $\text{Eu}^{3+}$  complexes with 1:1 stoichiometry. Among the complexes examined, the  $2\text{-Eu}^{3+}$  complex sensed the  $\text{NO}_3^-$  anion with the highest selectivity. Because these lanthanide complexes are superior to organic fluorescent receptors on account of their long-lived, line-shaped, and position-defined luminescence properties, it was concluded that the tripod provided an effective basis for the development of anion-responsive, luminescent lanthanide complexes.<sup>[20]</sup>

## Experimental Section

**General:**  $^1\text{H}$  and  $^{13}\text{C}$  NMR spectra were recorded on JEOL LA-300 and 400 spectrometers. Luminescence spectra were obtained on a Perkin–Elmer LS-50B equipped with a Hamamatsu R-928 photomultiplier. UV/Vis spectra were recorded with a Hitachi U-3500 apparatus. The  $\text{CH}_3\text{CN}$  employed for titration and luminescence experiments was purchased from Nacalai Tesque (spectroscopic analysis grade). Karl Fischer water determinations, carried out by UBE Scientific Analysis Laboratory (Ube, Japan), indicated that the solutions in  $\text{CH}_3\text{CN}$  contained 0.07–0.15 wt % of  $\text{H}_2\text{O}$ .  $\text{La}(\text{NO}_3)_3 \cdot 6\text{H}_2\text{O}$  and  $\text{Eu}(\text{NO}_3)_3 \cdot 6\text{H}_2\text{O}$  were purchased from Nacalai Tesque, and  $\text{Tb}(\text{NO}_3)_3 \cdot 6\text{H}_2\text{O}$  was purchased from Mitsuwa Chemicals.  $\text{La}(\text{CF}_3\text{SO}_3)_3$ ,  $\text{Eu}(\text{CF}_3\text{SO}_3)_3$ , and  $\text{Tb}(\text{CF}_3\text{SO}_3)_3$  were purchased from Sigma-Aldrich Japan K.K. These lanthanide salts were employed as received without further purification. Because 1:1:3 (tripod/ $\text{La}^{3+}/\text{NO}_3^-$ ) complexes were obtained from  $\text{CH}_3\text{CN}$  solutions, the  $\text{NO}_3^-$  anion provided stronger coordination with the lanthanide centers than contaminant water molecules.

**Tripods:** New tripods were synthesized as shown in Scheme 2 and fully characterized as described below.

**Tripod 2:** This ligand was derived from glycine amide and formyl pyridine. A mixture of *N,N*-diethylglycine amide hydrochloride (486 mg) and 2-pyridinecarboxaldehyde (938 mg) in MeOH (20 mL) was stirred at RT for 3 h under  $\text{N}_2$ . After cooling to  $0^\circ\text{C}$ ,  $\text{NaBH}_3\text{CN}$  (660 mg) in MeOH (10 mL) was slowly added to the mixture. After stirring for 60 h at RT, MeOH was evaporated, and the residue was dissolved in AcOEt, washed with saturated aqueous  $\text{NaHCO}_3$ , and dried over  $\text{Na}_2\text{SO}_4$ . The mixture was purified by column chromatography (alumina, EtOAc/hexane 8:2); to give **2** as a yellow oil (274 mg, 30%).  $R_f = 0.26$  (EtOAc/hexane 8:2);  $^1\text{H}$  NMR (400 MHz,  $\text{CDCl}_3$ ,  $25^\circ\text{C}$ , TMS):  $\delta = 8.53$  (dd, 2H,  $^3J(\text{H,H}) = 5.4$  Hz,  $^4J(\text{H,H}) = 1.8$  Hz; Ar), 7.65 (td, 2H,  $^3J(\text{H,H}) = 7.6$  Hz,  $^4J(\text{H,H}) = 1.7$  Hz; Ar), 7.58 (d, 2H,  $^3J(\text{H,H}) = 7.8$  Hz; Ar), 7.15 (t,  $^3J(\text{H,H}) = 5.4$  Hz, 2H; Ar), 3.94 (s, 4H;  $\text{ArCH}_2$ ), 3.41 (s, 2H;  $\text{CH}_2\text{CO}$ ), 3.34 (q,  $^3J(\text{H,H}) = 7.1$  Hz, 2H;  $\text{CH}_2\text{CH}_3$ ), 3.22 (q,  $^3J(\text{H,H}) = 7.1$  Hz, 2H;  $\text{CH}_2\text{CH}_3$ ), 1.09 (t,  $^3J(\text{H,H}) = 7.1$  Hz, 3H;  $\text{CH}_2\text{CH}_3$ ), 0.97 ppm (t,  $^3J(\text{H,H}) = 7.1$  Hz, 3H;  $\text{CH}_2\text{CH}_3$ );  $^{13}\text{C}$  NMR (100 MHz,  $\text{CDCl}_3$ ,  $25^\circ\text{C}$ ,  $\text{CHCl}_3$ ):  $\delta = 169.3$ , 159.2, 149.0, 136.5, 123.7, 122.1, 60.5, 55.3, 41.2, 40.1, 14.1, 13.0 ppm; IR (KBr):  $\tilde{\nu} = 1634$ ,  $767 \text{ cm}^{-1}$ ; HRMS (EI):  $m/z$ : calcd for  $\text{C}_{18}\text{H}_{24}\text{N}_4\text{O}$  [ $M$ ] $^+$ : 312.1950; found: 312.1953.

**Tripod 3:** This ligand was similarly prepared from glycine amide and formyl thiazole (14%). Yellow oil;  $R_f = 0.29$  (EtOAc/hexane 1:2);  $^1\text{H}$  NMR (400 MHz,  $\text{CDCl}_3$ ,  $25^\circ\text{C}$ , TMS)  $\delta = 7.72$  (d,  $^3J(\text{H,H}) = 3.2$  Hz, 2H; Ar), 7.31 (d,  $^3J(\text{H,H}) = 3.2$  Hz, 2H; Ar), 4.29 (s, 4H;  $\text{ArCH}_2$ ), 3.55 (s, 2H,  $\text{CH}_2\text{CO}$ ), 3.37 (q,  $^3J(\text{H,H}) = 7.1$  Hz, 2H;  $\text{CH}_2\text{CH}_3$ ), 3.20 (q,  $^3J(\text{H,H}) = 7.1$  Hz, 2H;  $\text{CH}_2\text{CH}_3$ ), 1.11 (t,  $^3J(\text{H,H}) = 7.1$  Hz, 3H;  $\text{CH}_2\text{CH}_3$ ), 1.04 ppm (t,  $^3J(\text{H,H}) = 7.1$  Hz, 3H;  $\text{CH}_2\text{CH}_3$ );  $^{13}\text{C}$  NMR (100 MHz,  $\text{CDCl}_3$ ,  $25^\circ\text{C}$ ,  $\text{CHCl}_3$ ):  $\delta = 170.2$ , 168.4, 142.5, 119.7, 55.7, 54.2, 41.2, 40.1, 14.1, 13.0 ppm; IR (KBr):  $\tilde{\nu} = 1639$ ,  $773 \text{ cm}^{-1}$ ; HRMS (EI):  $m/z$ : calcd for  $\text{C}_{14}\text{H}_{20}\text{N}_4\text{OS}_2$  [ $M$ ] $^+$ : 324.1078; found 324.1069.

**Tripod 4:** This ligand was obtained by treating pyrazine-ethanol mesylate with glycine amide. Pyrazine ethanol (1.45 g) in dry  $\text{CH}_2\text{Cl}_2$  (30 mL) was cooled to  $-15^\circ\text{C}$  under  $\text{N}_2$ . Triethylamine (1.74 g) was added and stirred for 5 min. Mesyl chloride (1.58 g) in dry  $\text{CH}_2\text{Cl}_2$  (10 mL) was slowly added to the solution. After stirring for 2 h, the temperature was slowly raised to  $0^\circ\text{C}$ . The reaction mixture was poured onto ice and extracted with  $\text{CH}_2\text{Cl}_2$ . The colorless oil turned black within 1 h and was then used without further purification and characterization. Pyrazine mesylate was dissolved in dry  $\text{CH}_3\text{CN}$  (30 mL). *N,N*-Diethylglycine amide hydrochloride (63 mg) and  $\text{K}_2\text{CO}_3$  (3.6 g) were added, and the mixture was heated at reflux for 18 h under  $\text{N}_2$ . The reaction mixture was filtered and the inorganic salt was washed thoroughly with  $\text{CH}_3\text{CN}$ . The filtrate and washing liquor were combined and evaporated. The residue was purified by GPC (1H-2H JAIGEL,  $\text{CHCl}_3$ ) followed by silica gel chromatography to give **4** as a yellow oil (83 mg, 70%).  $^1\text{H NMR}$  (400 MHz,  $\text{CDCl}_3$ ,  $25^\circ\text{C}$ , TMS):  $\delta$  = 8.74 (brd,  $^4J(\text{H,H}) = 1.2$  Hz, 2H; Ar), 8.51 (dd,  $^3J(\text{H,H}) = 2.4$  Hz,  $^4J(\text{H,H}) = 1.2$  Hz, 2H; Ar), 8.46 (brd,  $^3J(\text{H,H}) = 2.4$  Hz, 2H; Ar), 4.09 (s, 4H;  $\text{ArCH}_2$ ), 3.50 (s, 2H;  $\text{CH}_2\text{CO}$ ), 3.36 (q,  $^3J(\text{H,H}) = 7.2$  Hz, 2H;  $\text{CH}_2\text{CH}_3$ ), 3.20 (q,  $^3J(\text{H,H}) = 7.2$  Hz, 2H;  $\text{CH}_2\text{CH}_3$ ), 1.11 (t,  $^3J(\text{H,H}) = 7.2$  Hz, 3H;  $\text{CH}_2\text{CH}_3$ ), 1.02 ppm (t,  $^3J(\text{H,H}) = 7.2$  Hz, 3H;  $\text{CH}_2\text{CH}_3$ );  $^{13}\text{C NMR}$  (100 MHz,  $\text{CDCl}_3$ ,  $25^\circ\text{C}$ ,  $\text{CHCl}_3$ ):  $\delta$  = 168.7, 154.5, 145.5, 143.8, 143.2, 57.9, 55.2, 41.2, 40.1, 14.1, 13.0 ppm; IR (KBr):  $\tilde{\nu}$  = 1643, 1579, 1527, 1464, 1435, 1019  $\text{cm}^{-1}$ ; HRMS (EI):  $m/z$ : calcd for  $\text{C}_{16}\text{H}_{22}\text{N}_6\text{O}$  [ $M$ ] $^+$ : 314.1854; found 314.1855.

**Tripod 5:**<sup>[10]</sup> Colorless crystals (hexane);  $R_f = 0.16$  (33% EtOAc in hexane);  $^1\text{H NMR}$  (400 MHz,  $\text{CDCl}_3$ ,  $25^\circ\text{C}$ , TMS):  $\delta$  = 8.12 (d,  $^3J(\text{H,H}) = 8.6$  Hz, 2H; Ar), 8.05 (d,  $^3J(\text{H,H}) = 8.6$  Hz, 2H; Ar), 7.82–7.66 (m, 4H; Ar), 7.68 (td,  $J = 8.6, 1.3$  Hz, 2H; Ar), 7.51 (td,  $J = 8.6, 1.3$  Hz, 2H; Ar), 4.12 (s, 4H;  $\text{ArCH}_2$ ), 3.51 (s, 2H;  $\text{CH}_2\text{CO}$ ), 3.40 (q,  $^3J(\text{H,H}) = 7.1$  Hz, 2H;  $\text{CH}_2\text{CH}_3$ ), 3.24 (q,  $^3J(\text{H,H}) = 7.1$  Hz, 2H;  $\text{CH}_2\text{CH}_3$ ), 1.07 (t,  $^3J(\text{H,H}) = 7.1$  Hz, 3H;  $\text{CH}_2\text{CH}_3$ ), 0.93 ppm (t,  $^3J(\text{H,H}) = 7.1$  Hz, 3H;  $\text{CH}_2\text{CH}_3$ );  $^{13}\text{C NMR}$  (100 MHz,  $\text{CDCl}_3$ ,  $25^\circ\text{C}$ ,  $\text{CHCl}_3$ ):  $\delta$  = 169.2, 160.1, 147.6, 136.3, 129.3, 129.1, 127.5, 127.4, 126.2, 121.9, 61.4, 55.6, 41.2, 40.1, 14.1, 13.0 ppm; IR (KBr):  $\tilde{\nu}$  = 1656, 773  $\text{cm}^{-1}$ ; elemental analysis calcd (%) for  $\text{C}_{26}\text{H}_{28}\text{N}_4\text{O}$  (412.5): C 75.70, H 6.84, N 13.58; found: C 75.43, H 6.89, N 13.43.

**Tripod 6:** This ligand was synthesized by treating 2-aminomethylpyridine with diethyl chloroacetamide. A mixture of 2-aminomethylpyridine (432 mg), diethyl chloroacetamide (1.56 g), and  $\text{Na}_2\text{CO}_3$  (2.12 g) in  $\text{CH}_3\text{CN}$  (60 mL) was heated at reflux for 7 h under  $\text{N}_2$ .  $\text{CH}_3\text{CN}$  was evaporated, and the residue was dissolved in  $\text{CH}_2\text{Cl}_2$  and filtered. The filtrate was purified by column chromatography (alumina, EtOAc) to give **6** as a yellow oil (855 mg, 64%).  $R_f = 0.37$  (EtOAc);  $^1\text{H NMR}$  (400 MHz,  $\text{CDCl}_3$ ,  $25^\circ\text{C}$ , TMS):  $\delta$  = 8.52 (dd,  $^3J(\text{H,H}) = 5.0$  Hz,  $^4J(\text{H,H}) = 1.4$  Hz, 1H; Ar), 7.69–7.64 (m, 2H; Ar), 7.16 (td,  $^3J(\text{H,H}) = 5.0$  Hz,  $^4J(\text{H,H}) = 2.7$  Hz, 1H; Ar), 3.98 (s, 2H;  $\text{ArCH}_2$ ), 3.55 (s, 4H;  $\text{CH}_2\text{CO}$ ), 3.35 (q,  $^3J(\text{H,H}) = 7.1$  Hz, 4H;  $\text{CH}_2\text{CH}_3$ ), 3.27 (q,  $^3J(\text{H,H}) = 7.1$  Hz, 4H;  $\text{CH}_2\text{CH}_3$ ), 1.10 (t,  $^3J(\text{H,H}) = 7.1$  Hz, 6H;  $\text{CH}_2\text{CH}_3$ ), 1.06 ppm (t,  $^3J(\text{H,H}) = 7.1$  Hz, 6H;  $\text{CH}_2\text{CH}_3$ );  $^{13}\text{C NMR}$  (100 MHz,  $\text{CDCl}_3$ ,  $25^\circ\text{C}$ ,  $\text{CHCl}_3$ ):  $\delta$  = 169.5, 159.3, 148.8, 136.5, 124.1, 122.1, 60.8, 55.6, 41.4, 40.1, 14.2, 13.1 ppm; IR (KBr):  $\tilde{\nu}$  = 1635, 771  $\text{cm}^{-1}$ ; HRMS (EI):  $m/z$ : calcd for  $\text{C}_{18}\text{H}_{30}\text{N}_4\text{O}_2$  [ $M$ ] $^+$ : 334.2369; found 334.2369.

**X-Ray crystal structure determination:** A single crystal of the  $[\text{La}(\mathbf{2})\text{(NO}_3)_3]$  complex was recrystallized from  $\text{CH}_3\text{CN}$ /hexane, mounted in inert oil, and transferred to the cold gas stream of the diffractometer ( $-150^\circ\text{C}$ ). X-ray data were collected with graphite-monochromated  $\text{MoK}\alpha$  radiation (0.71070 Å) on a Rigaku/MS Mercury CCD system. The structure was solved by the heavy-atom Patterson method (DIRDIF-99)<sup>[21]</sup> and expanded with Fourier techniques. The non-hydrogen atoms were refined anisotropically by the full-matrix least-squares method of SHELXL-97.<sup>[22]</sup> Hydrogen atoms were located on calculated positions and were not refined.

*Crystal data for the tripod  $[\text{La}(\mathbf{2})\text{(NO}_3)_3]$  complex:*<sup>[23]</sup>  $\text{C}_{27}\text{H}_{28.5}\text{LaN}_{8.5}\text{O}_{10}$ ;  $M = 698.93$ ; crystal size  $0.15 \times 0.15 \times 0.10$  mm<sup>3</sup>; monoclinic;  $a = 40.202(4)$ ,  $b = 8.4382(5)$ ,  $c = 19.6041(16)$  Å;  $\beta = 116.997(3)^\circ$ ;  $V = 5925.6(8)$  Å<sup>3</sup>;  $T = 123$  K; space group  $C2/c$  (no. 15);  $Z = 8$ ;  $\rho_{\text{calcd}} = 1.567$  Mg m<sup>-3</sup>; absorption coefficient =  $1.505$  mm<sup>-1</sup>;  $F(000) = 2808$ ;  $\theta$  range for data collection:  $3.02$  to  $27.48^\circ$ ; reflections collected: 21238, independent reflections: 6404

( $R_{\text{int}} = 0.0397$ ); completeness to  $\theta = 27.48^\circ$ : 94.3%; max. and min. transmission: 0.8640 and 0.8057; data/restraints/parameters: 6404/0/353; goodness-of-fit on  $F^2$ : 1.280; final  $R$  values were  $R1 = 0.0557$  and  $wR2 = 0.1248$  (all data) and  $R1 = 0.0517$  and  $wR2 = 0.1215$  [ $I > 2\sigma(I)$ ].

**EXAFS measurements and data analyses:** The EXAFS spectra at the  $K$ -edge of La (38.9 keV) were measured in the fluorescence mode with a 19-element Ge array detector at the BL11XU of SPring-8, Japan. Synchrotron radiation was monochromatized with a double crystal Si(333) monochromator cooled by liquid nitrogen. Movement of the insertion device was synchronized with monochromator scanning. EXAFS data reduction and curve fitting were carried out by the data analysis package WinXAS 3.0 (Ressler, 1997). Theoretical phases and backscattering amplitude for curve fitting were calculated by FEFF 8.02 (Zabinsky, 1995) on the basis of the coordinates from X-ray crystallography. The solution of the  $[\text{La}(\mathbf{2})\text{(NO}_3)_3]$  complex ( $5.00 \times 10^{-3}$  mol L<sup>-1</sup>) in  $\text{CH}_3\text{CN}$  was sealed in a polyethylene bag, whereas the crystal sample mixed with boron nitrate was shaped into a disc form (approximately 5 mm diameter and 1 mm thickness) by a forming holder and a hydraulic compactor.

**Computational details:** The basis sets used in our quantum chemical calculations were Stuttgart-RSC-ECP (relativistic small-core effective core potential)<sup>[24]</sup> for La and cc-pVDZ<sup>[25]</sup> for the other atoms (C, N, O, and H). Scalar relativistic effects, which are important for the determination of the electronic structure of heavy elements (such as La) systems, were included through ECP Natural bond orbital (NBO) analyses<sup>[16]</sup> were performed with the optimized geometries to investigate charge distributions in the  $\text{La}(\text{NO}_3)_3$  complexes and to understand interactions between  $\text{La}(\text{NO}_3)_3$  and tripods **2**, **3**, **4**, and **5**. All of the B3LYP calculations were performed with the Gaussian 03<sup>[26]</sup> quantum chemical program package.

**Titration experiments:** More than fifteen samples with different ratios of tripod to lanthanide salt were prepared in each titration experiment. Typically, a solution (5 mL) in  $\text{CH}_3\text{CN}$  containing tripod **2** ( $2.00 \times 10^{-4}$  mol L<sup>-1</sup>) and lanthanide salt ( $0$ – $6.00 \times 10^{-4}$  mol L<sup>-1</sup>) was prepared and stirred for 5 min before starting the measurements. The absorbance values of the aromatic nitrogen chromophores were plotted against the mole ratios of the tripod to the lanthanide cation and the stepwise  $\log K$  values were calculated. The calculations were performed with IGOR Pro (version 4, WaveMetrics). Although the standard deviations of the estimated  $\log K$  values are within 0.01, two independent results were averaged; their error ranges are shown in Table 2.

**Luminescence experiments:** The luminescence experiments of the  $\text{Eu}^{3+}$  and  $\text{Tb}^{3+}$  complexes were performed in  $\text{CH}_3\text{CN}$  upon ligand excitation: 261 nm for tripod **2**, 246 nm for tripod **3**, 270 nm for tripod **4**, and 305 nm for tripod **5**. The concentrations of the lanthanide salts and the tripods as well as the other conditions are shown in each figure. Because lanthanide complexation offered slight UV/Vis spectral changes, the ligand-excitation luminescence spectra recorded were normalized by absorbance in the excitation region.

The indicated lifetimes ( $\tau$ ) are the averaged values of at least three independent measurements, each of which was made by monitoring the emission intensity at 616 nm (for  $\text{Eu}^{3+}$ ) or 543 nm (for  $\text{Tb}^{3+}$ ) after twenty different delay times spanning a range of at least two lifetimes ( $\lambda_{\text{ex}} = 261$  nm for tripod **2** and 270 nm for tripod **4**). Slit widths of 10 nm were used and the gate time was 0.1 ms. The decay curves were fitted by an equation of the form  $I(t) = I(0)\exp(-t/\tau)$  with a curve-fitting program. A high correlation coefficient was observed in each case.

## Acknowledgements

This work was supported by a Grants-in-Aid for Scientific Research (Nos. 16080217 and 17350030) from The Ministry of Education, Culture, Sports, Science, and Technology (Japan). The authors are grateful to Dr. T. Kimura of Japan Atomic Energy Research Institute for helpful suggestions regarding lanthanide complexation.



- [1] a) "Frontiers in Lanthanide Chemistry" (Thematic Issue): *Chem. Rev.* **2002**, *102*, 1805–2476; b) "Lanthanide Compounds for Therapeutic and Diagnostic Applications" (Thematic Issue): *Chem. Soc. Rev.* **2006**, *35*, 499–571.
- [2] For reviews, see: a) J.-C. G. Bünzli, C. Piguet, *Chem. Soc. Rev.* **2005**, *34*, 1048–1077; b) D. Fiedler, D. H. Leung, R. G. Bergman, K. N. Raymond, *Acc. Chem. Res.* **2005**, *38*, 349; c) M. Shibasaki, *Proc. Jpn. Acad. Ser. B* **2006**, *62*, 72–85.
- [3] Reviews: a) T. Gunnlaugsson, J. P. Leonard, *Chem. Commun.* **2005**, 3114–3131; b) S. Pandya, J. Yu, D. Parker, *Dalton Trans.* **2006**, 2757–2766; c) S. Shinoda, H. Miyake, H. Tsukube in *Handbook on the Physics and Chemistry of Rare Earths, Vol. 35* (Eds.: K. A. Gschneider, Jr., J.-C. G. Bünzli, V. K. Pecharsky), Elsevier, **2005**, pp. 273–375; for recent examples, see: d) L. J. Charbonnière, R. Schurhammer, S. Mameri, G. Wipff, R. F. Ziessel, *Inorg. Chem.* **2005**, *44*, 7151–7160; e) M. D. Best, E. V. Anslyn, *Chem. Eur. J.* **2003**, *9*, 51–57; f) N. W. Luedtke, A. Schepartz, *Chem. Commun.* **2005**, 5426–5428; g) R. J. Aarons, J. K. Notta, M. M. Meloni, J. Feng, R. Vidyasagar, J. Narvainen, S. Allan, N. Spencer, R. A. Kaupinen, J. S. Snaith, S. Faulkner, *Chem. Commun.* **2006**, 909–911; h) S. Balakrishnan, N. J. Zondlo, *J. Am. Chem. Soc.* **2006**, *128*, 5590–5591; i) T. Terai, K. Kikuchi, S. Iwasawa, T. Kawabe, Y. Hirata, Y. Urano, T. Nagano, *J. Am. Chem. Soc.* **2006**, *128*, 6938–6946; j) B. R. Sculimbrene, B. Imperiali, *J. Am. Chem. Soc.* **2006**, *128*, 7346–7352.
- [4] a) V. Vicinelli, P. Ceroni, M. Maestri, V. Balzani, M. Gorka, F. Vögtle, *J. Am. Chem. Soc.* **2002**, *124*, 6461–6468; b) J. P. Cross, M. Lauz, P. D. Badger, S. Petoud, *J. Am. Chem. Soc.* **2004**, *126*, 16278–16279; c) H. Tsukube, Y. Suzuki, D. Paul, Y. Kataoka, S. Shinoda, *Chem. Commun.* **2007**, 2533–2535.
- [5] a) L. Natrajan, J. Pécaut, M. Mazzanti, C. LeBrun, *Inorg. Chem.* **2005**, *44*, 4756–4765; b) S. Yamada, S. Shinoda, H. Tsukube, *Chem. Commun.* **2002**, 1218–1219; c) T. Yamada, S. Shinoda, H. Sugimoto, J. Uenishi, H. Tsukube, *Inorg. Chem.* **2003**, *42*, 7932–7937.
- [6] a) T. Yaita, S. Tachimori, N. M. Edelstein, J. J. Bucher, L. Rao, D. K. Shuh, *J. Synchrotron Radiat.* **2001**, *8*, 663–665; b) T. Yaita, H. Shiwaku, S. Suzuki, Y. Okamoto, A. Shimada, Z. Assefa, R. G. Haire, *Phys. Scr.* **2005**, 302–305; c) R. O. Freire, G. B. Rocha, A. M. Simas, *Inorg. Chem.* **2005**, *44*, 3299–3310; d) T. Kajiwarra, K. Katagiri, M. Hasegawa, A. Ishii, M. Ferbinteanu, S. Takaishi, T. Ito, M. Yamashita, N. Iki, *Inorg. Chem.* **2006**, *45*, 4880–4882; e) K. Sénéchal-David, A. Hemeryck, N. Tancrez, L. Toupet, J. A. G. Williams, I. Ledoux, J. Zyss, A. Boucekkinne, J.-P. Guégan, H. Le Bozec, O. Maury, *J. Am. Chem. Soc.* **2006**, *128*, 12243–12255; f) M. González-Lorenzo, C. Platas-Iglesias, F. Aveccilla, S. Faulkner, S. J. A. Pope, A. de Blas, T. Rodríguez-Blas, *Inorg. Chem.* **2005**, *44*, 4254–4262.
- [7] a) X.-P. Yang, C.-Y. Su, B.-S. Kang, X.-L. Feng, W.-L. Xiao, H.-Q. Liu, *J. Chem. Soc. Dalton Trans.* **2000**, 3253–3260; b) M. Mazzanti, R. Wietzke, J. Pécaut, J.-M. Latour, P. Maldivi, M. Remy, *Inorg. Chem.* **2002**, *41*, 2389–2399; c) B. M. Flanagan, P. V. Bernhardt, E. R. Krausz, S. R. Lüthi, M. J. Riley, *Inorg. Chem.* **2002**, *41*, 5024–5033.
- [8] X.-P. Yang, B.-S. Kang, W.-K. Wong, C.-Y. Su, H.-Q. Liu, *Inorg. Chem.* **2003**, *42*, 169–179.
- [9] a) R. Wietzke, M. Mazzanti, J.-M. Latour, J. Pécaut, *Chem. Commun.* **1999**, 209–210; b) C.-Y. Su, B.-S. Kang, H.-Q. Liu, Q.-G. Wang, Z.-N. Chen, Z.-L. Lu, Y.-X. Tong, T. C. W. Mak, *Inorg. Chem.* **1999**, *38*, 1374–1375; c) X.-L. Zheng, Y. Liu, M. Pan, X.-Q. Lü, J.-Y. Zhang, C.-Y. Zhao, Y.-X. Tong, C.-Y. Su, *Angew. Chem.* **2007**, *119*, 7543–7547; *Angew. Chem. Int. Ed.* **2007**, *46*, 7399–7403.
- [10] Preliminary results of tripod 5-lanthanide complexation were presented at the 10th International Meeting on Chemical Sensors, see: a) Y. Kataoka, S. Shinoda, H. Miyake, H. Tsukube, *Chem. Sensors* **2004**, *20B*, 484–485; its chiral derivatives were also prepared, see: b) Y. Kataoka, D. Paul, H. Miyake, S. Shinoda, H. Tsukube, *Dalton Trans.* **2007**, 2784–2791.
- [11] S. Comby, J.-C. G. Bünzli in *Handbook on the Physics and Chemistry of Rare Earths, Vol. 37* (Eds.: K. A. Gschneider, Jr., J.-C. G. Bünzli, V. K. Pecharsky), Elsevier, Amsterdam, **2007**, pp. 217–470.
- [12] L. Karmazin, M. Mazzanti, C. Gateau, C. Hill, J. Pecaut, *Chem. Commun.* **2002**, 2892–2893.
- [13] a) C. Paul-Roth, K. N. Raymond, *Inorg. Chem.* **1995**, *34*, 1408–1412; b) S. C. Burdette, C. J. Frederickson, W. Bu, S. J. Lippard, *J. Am. Chem. Soc.* **2003**, *125*, 1778–1787.
- [14] N. Nakamura, Y. Hasegawa, H. Kawai, N. Yasuda, N. Kanahisa, Y. Kai, T. Nagamura, S. Yanagida, Y. Wada, *J. Phys. Chem. A* **2007**, *111*, 3029–3037.
- [15] a) M. T. Cancès, B. Mennucci, J. Tomasi, *J. Chem. Phys.* **1997**, *107*, 3032–3041; b) M. Cossi, V. Barone, B. Mennucci, J. Tomasi, *Chem. Phys. Lett.* **1998**, *286*, 253–260; c) B. Mennucci, J. Tomasi, *J. Chem. Phys.* **1997**, *106*, 5151–5158.
- [16] A. E. Reed, L. A. Curtiss, F. Weinhold, *Chem. Rev.* **1988**, *88*, 899–926.
- [17] R. M. Izatt, K. Pawlak, J. S. Bradshaw, R. L. Bruening, *Chem. Rev.* **1991**, *91*, 1721–2085.
- [18] a) J. H. Forsberg, *Coord. Chem. Rev.* **1973**, *10*, 195–226; b) L. I. Katzin, *Inorg. Chem.* **1969**, *8*, 1649–1654.
- [19] Without additives, the luminescence lifetimes for the equimolar mixtures of Eu(OTf)<sub>3</sub> and tripods were 1.0 ms (**2**) and 0.8 ms (**4**).
- [20] Luminescent lanthanide complexes have a wide range of applications as smart probes for biological imaging, for examples, see: a) S. Faulkner, S. J. A. Pope, *J. Am. Chem. Soc.* **2003**, *125*, 10526–10527; b) S. Quici, M. Cavazzini, G. Marzanni, G. Accorsi, N. Armaroli, B. Ventura, F. Barigelletti, *Inorg. Chem.* **2005**, *44*, 529–537; c) D. Imbert, S. Comby, A.-S. Chauvin, J.-C. G. Bünzli, *Chem. Commun.* **2005**, 1432–1434; d) R. F. Ziessel, G. Ulrich, L. Charbonnière, D. Imbert, R. Scopelliti, J.-C. G. Bünzli, *Chem. Eur. J.* **2006**, *12*, 5060–5067.
- [21] P. T. Beurskens, G. Beurskens, R. de Gelder, S. Garcia-Granda, R. O. Gould, R. Israel, J. M. M. Smits, The DIRDIF-99 program system, Crystallography Laboratory, University of Nijmegen (The Netherlands), **1999**.
- [22] G. M. Sheldrick, *SHELXL-97*, Program for the Refinement of Crystal Structures, University of Göttingen, Göttingen (Germany), **1997**.
- [23] CCDC-643580 contains the supplementary crystallographic data for this paper. These data can be obtained free of charge from The Cambridge Crystallographic Data Centre via [www.ccdc.cam.ac.uk/data\\_request/cif](http://www.ccdc.cam.ac.uk/data_request/cif).
- [24] X. Cao, M. Dolg, *J. Chem. Phys.* **2001**, *115*, 7348–7355.
- [25] T. H. Dunning, Jr., *J. Chem. Phys.* **1989**, *90*, 1007–1023.
- [26] Gaussian 03, Revision B.04, M. J. Frisch, G. W. Trucks, H. B. Schlegel, G. E. Scuseria, M. A. Robb, J. R. Cheeseman, J. A. Montgomery, Jr., T. Vreven, K. N. Kudin, J. C. Burant, J. M. Millam, S. S. Iyengar, J. Tomasi, V. Barone, B. Mennucci, M. Cossi, G. Scalmani, N. Rega, G. A. Petersson, H. Nakatsuji, M. Hada, M. Ehara, K. Toyota, R. Fukuda, J. Hasegawa, M. Ishida, T. Nakajima, Y. Honda, O. Kitao, H. Nakai, M. Klene, X. Li, J. E. Knox, H. P. Hratchian, J. B. Cross, V. Bakken, C. Adamo, J. Jaramillo, R. Gomperts, R. E. Stratmann, O. Yazyev, A. J. Austin, R. Cammi, C. Pomelli, J. W. Ochterski, P. Y. Ayala, K. Morokuma, G. A. Voth, P. Salvador, J. J. Dannenberg, V. G. Zakrzewski, S. Dapprich, A. D. Daniels, M. C. Strain, O. Farkas, D. K. Malick, A. D. Rabuck, K. Raghavachari, J. B. Foresman, J. V. Ortiz, Q. Cui, A. G. Baboul, S. Clifford, J. Cioslowski, B. B. Stefanov, G. Liu, A. Liashenko, P. Piskorz, I. Komaromi, R. L. Martin, D. J. Fox, T. Keith, M. A. Al-Laham, C. Y. Peng, A. Nanayakkara, M. Challacombe, P. M. W. Gill, B. Johnson, W. Chen, M. W. Wong, C. Gonzalez, J. A. Pople, Gaussian, Inc., Wallingford CT, **2004**.

Received: December 3, 2007  
Published online: April 30, 2008